

Friction Behavior of Anodic Oxide Layer Coating on 2017A T4 Aluminum Alloy under Severe Friction Solicitation: The Effect of Anodizing Parameters

Mohamed Kchaou

Department of Mechanical Engineering, College of Engineering, University of Bisha, P.O. Box 001, Bisha, Saudi Arabia

kchaou.mohamed@yahoo.fr (corresponding author)

Received: 26 October 2023 | Revised: 13 November 2023 | Accepted: 27 November 2023

Licensed under a CC-BY 4.0 license | Copyright (c) by the authors | DOI: <https://doi.org/10.48084/etasr.6562>

ABSTRACT

This article aims to highlight the wear mechanisms and friction behavior of the 2017A T4 anodized aluminum alloy used for automotive and aerospace applications. The effect of the processing parameters on the durability of the anodized layer under high friction is studied. Scratch tests were carried out to study the level of the friction coefficient with the increase in the thickness of the oxide layer formed on the Al 2017 A (AU4G) substrate. The results of the scratch tests show that the variation in the anodization duration, which influences the thickness of the oxide layer, induces an increase in the coefficient of friction. Besides, the variations in friction coefficient with sliding distance are influenced by the changes in wear morphology and degree of oxidation. Treated surfaces with a thickness of 50 μm have the lowest friction coefficients and wear rates. Their improved wear resistance may be related to the increased bond strength compared to other anodized surfaces. The tribological damage was characterized by the detachment of debris, which increases with the increase of the duration of anodization. Upon sliding, its detachment leads to delamination of the underlying anodic aluminum oxides and subsequent abrasion of the aluminum substrate.

Keywords-aluminum alloy; anodizing parameters; layer thickness; friction; damage; static and cyclic friction

I. INTRODUCTION

Due to the dynamic and quick development of the automotive and aerospace industries, in mechanical parts (motors, assembly elements, struts, turbine rotor, etc.) or complex tools (carbon fiber draping mold for the manufacture of aircraft doors, etc.) increasing demands, such as safety, reliability, performance, weight reduction, sustainable process, cannot be met by traditional materials, especially when the system is submitted to high mechanical, thermal, and chemical solicitation [1-4]. Aluminum alloys can be a suitable alternative to the materials supporting different types of in-service load [5-7]. They are manufactured in 8 series with hundreds of different specific chemical compositions [8]. The coating of aluminum and its alloys are widely used for its quality of finish and its applications are expanding in various fields, particularly in the transport sector. In the case of anodized aluminum alloys, the damage modes of the layer are mostly in their appearance, source, and category according to the stage of production, but also to the choice of the elaboration parameters [9, 10]. Most damage modes are surface (corrosion, streaking defect, non-uniform appearance, deterioration defects), mechanical (damage due to tensile and bending stress), and

tribological (wear and scratch, fatigue) failure modes [11-16]. The alumina layer which is obtained generally by applying an electrical current and immersing the piece in acid solution is the first body exposed to the tribological damage when the material is solicited in friction [17]. The most widely used high strength aluminum alloys in the aerospace and automotive industries are the 2000 series. However, the main additive component in this alloy, namely the copper, disrupts the formation of the anodic layer and destroys the wear resistance [18-20]. The thickness of the oxide layer is of the order of a few microns. The morphology of this layer comprises a thin barrier layer at the oxide/substrate interface and a thicker porous layer to the outside [18]. Reliable and safe performance of aluminum parts requires a sufficiently accurate assessment of the durability of the alloys. The value of the coefficient of friction and the stability and wear mechanisms are the most important properties for evaluating the friction performance of materials. Many researchers have used tribological tests, such as cyclic resistance tests, to demonstrate the abrasion resistance of anodized aluminum and to examine wear properties and the friction coefficient. Authors in [21] studied the effect of the residual stress on the friction and wear properties has been analyzed. Authors in [20] reported that increasing the thickness

of the anodic coating increased both the compressive strength and the elastic modulus of AA3003 aluminum micro lattice. When studying the tribological properties of the anodic coatings by the dry friction test, authors in [23] noticed that the addition of Al_2O_3 and PTFE particles to the sulfuric-oxalic acid electrolyte resulted in hard anodic composite coatings with improved wear resistance. The results reported in [24] revealed that there was an optimum value for the electrolyte concentration, as well as the hard anodizing current density and the time at which the hardest coating was obtained for the anodized 6061-T6 series. Authors in [9] studied the AA5052 series immersed for 20 min in sulfuric acid solution. The results showed that their morphological and mechanical properties synergistically influenced the damage resistance. The interactions between the released supports and the porous surface changed and the released particles only had a lubricating effect, lowering the coefficient of friction and the wear rate. Authors in [25, 26] studied the effect of anodizing parameters of aluminum alloy EN AW-5251 on the thickness and roughness of Al_2O_3 layers as well as their wettability and tribological properties in sliding combination with the T7W material. The results showed that the anodizing parameters significantly affect the thickness of Al_2O_3 layers. The correlation analysis showed a significant relationship between the roughness parameters and the wettability of the surface of the layers, which affects the ability to create and maintain a sliding film.

Despite the number of studies regarding several parameters which can affect the friction behavior of the anodizing coating, very limited work has been conducted on the effect of anodizing parameters on the tribological failure under static and cyclic friction solicitation of the 2017A T4 aluminum alloys. In fact, in the majority of mechanical parts, the surface of anodized aluminum should resist to static friction (continue, intermittent, discontinue sliding), but also to cyclic loading such as reciprocating sliding, circular sliding, which can help designers in the choice of the suitable characteristics to assume the performance of the material in service. This study investigates the friction behavior of the anodized 2017A aluminum alloy for different conditions of anodization, in terms of coefficient of friction and scratch resistance. The effect of different anodizing parameters related to the applied current and anodizing duration on the tribological behavior of the material is highlighted both under static and cyclic loading. Observations are used to characterize the worn surface and to correlate the friction behavior to the wear mechanisms.

II. MATERIALS AND METHODS

A. Material

The investigated material is the 2017A-T4 aluminum alloy. The chemical composition of the anodized alloy is shown in Table I. All specimens (50 mm × 30 mm × 3 mm) were individually anodized. Table II shows the established anodizing parameters. Prior to anodizing, the specimens were subjected to different stages of surface preparation to eliminate the spontaneously formed layers:

- Mechanical polishing of grade P120 up to P1500. The objective is to have a smooth surface with low roughness in order to guarantee better surface quality.
- Rinsing with tap water to remove particles adhering to the surface from mechanical polishing.
- Degreasing to clean residual lubricant samples, grease, abrasive grains, and burrs. Degreasing provides a hydrophobic, stain-repellent surface.
- Pickling to eliminate the oxide layer obtained spontaneously on the surface. The pickling bath contains 60 g/l NaOH solution. The sample is immersed in the NaOH bath for 1 min at 60 °C.
- Bleaching to eliminate the blackening of aluminum by aluminum hydroxide. The sample is immersed in a solution of nitric acid (HNO_3) with a concentration of 200 g/l, at room temperature for 2 min.
- Electrochemical polishing to eliminate micro scratches and submicroscopic roughness from the alloy surface. The electro-polishing bath contains acetic acid ((CH_3COOH) 100%: 655 ml/l) and perchloric acid ($(HClO_4)$ 60%: 345 ml/l) at 20 °C. The treatment time is 2 min by applying a voltage of 10 V. The anodizing bath contains diluted sulfuric acid with agitation. A DC stabilizing generator is used to provide the anodizing current.

The experimental parameters i.e. applied current density, sulfuric acid concentration, and duration of anodization are listed in Table II. Three alloy samples were anodized in each experiment.

TABLE I. CHEMICAL COMPOSITION OF THE ALUMINIUM ALLOY 2017AT4

Element	Wt%
Si	0.66
Fe	0.40
Cu	4.3
Mn	0.6
Mg	0.74
Cr	0.04
Zn	0.19
Ti	0.05
Ti+Zr	0.06
Al	Rest

TABLE II. EXPERIMENTAL PARAMETERS

#	Duration of anodization (min)	Sulfuric acid concentration (g/l)	Applied current density (A/dm^2)	Anodizing bath temperature (°C)
1	30	100	1	15
2	60	100	2	15
3	30	200	2	15

B. Characterization Methods

1) Control of the Thickness of the Oxide Layer

Thickness control of the oxide layer was measured by the eddy current method (coating thickness gauge LPTOSKOP 2042). The principle is to apply a probe on the ideally clean,

flat, and low roughness surface of the coating to be measured. The value range of the thickness is a few micrometers.

2) Scratch Test

For the scratch machine, an indenter, of specific shape and hard material, moves with a constant speed on the surface of the sample by applying a constant normal force during the test. The scratch test was carried out dry on all the samples anodized by the different parameters presented in Table II, applying a load of 6.5 N for a scratch length of 20 mm with a speed of 105 mm/min. The shape of the indenter is conical with an angle of attack equal to 60° .

3) Cyclic Friction Test

The cyclic friction test was carried out under dry conditions in an ambient laboratory environment (25-27 °C) at a Relative Humidity (RH) of 63-67%. Stable sliding motions were applied with a speed of 10 mm/s with a stroke of 15 mm for up to 100 cycles. Friction tests were performed with applied load of 6.5 N and were carried out by a hard steel ball 100Cr6 at dry sliding.

III. RESULTS AND DISCUSSION

A. Topographical Analysis of the Coated Surface

Figure 1 shows the surface topography of the anodized surfaces for 30 and 60 min. It is clear that the surface is covered by well distributed oxides with more concentrated and accumulated particles for the 60 min sample. In fact, SEM observation of the surface of the samples shows non-homogeneous surfaces, with microcavities and individualized particles, but agglomerated and randomly distributed. Going from 30 to 60 min, the submicron-sized microcavities slightly increase in size. Their homogeneity improves by increasing the anodizing duration.

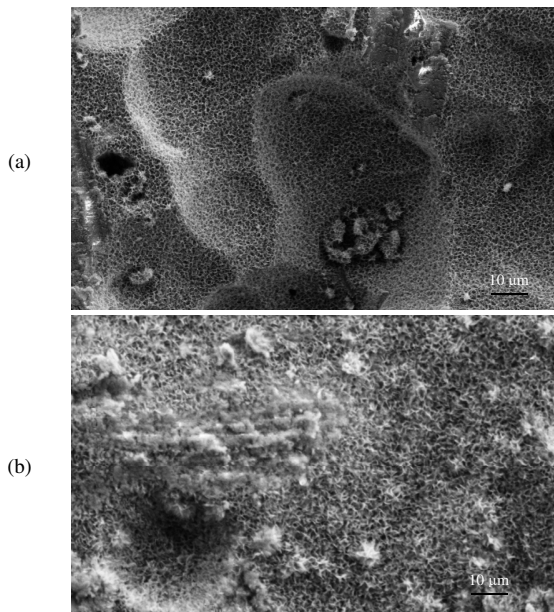


Fig. 1. Surface topography of the anodized aluminum alloys for: (a) 30 min and (b) 60 min anodization duration.

B. Influence of Anodizing Duration on the Thickness of the Oxide Layer

A typical in depth microstructure is a network of fine channels created from each discharge event [9]. The oxide coating generally consists of three layers: a barrier layer, an intermediate layer, and an outer layer. After the measurements made by the eddy current method, two ranges of measurements of the thickness of the oxide layer were distinguished. The illustration of the thickness for the 2 materials is given in Figure 2. For the sample 1 of the first experiment with 30 min immersion in the anodizing bath, a thickness of $9.5 \pm 0.5 \mu\text{m}$ of the oxide layer was found (Table III). On the other hand, concerning the sample 2 of the second experiment, the thickness of the oxide layer is equal to $12 \pm 0.5 \mu\text{m}$. However, other authors have shown that the surface roughness and the surface curvature have an influence on the value of the thickness of the oxide layer. Also, the contact pressure affects the measurement by the eddy current method [27].

TABLE III. AVERAGE THICKNESS FOR DIFFERENT ANODIZING PARAMETERS

No samples/duration	Sample 1/ 30 min	Sample 2/ 60 min
Average thickness (μm)	9.5	12

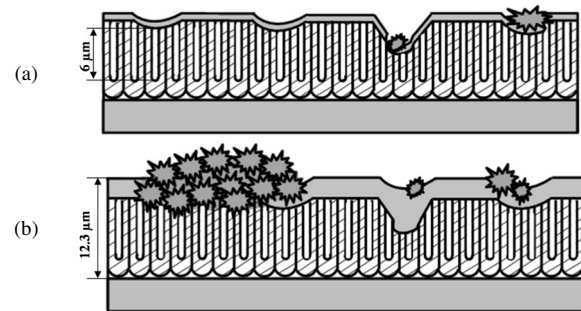


Fig. 2. Illustration of the thickness of the oxide layer for: (a) 30 min, (b) 60 min anodizing duration.

Authors in [28] studied the influence of anodizing time on the thickness of the oxide layer and its morphology using replica electron micrographs. They found that the diameter of the pores obtained by the sulfuric anodizing at the surface increases with anodizing time due to the dissolution by sulfuric acid. The increase in the anodizing time causes the growth of the thickness of the oxide layer which becomes a porous layer having a duplex structure consisting of a compact inner layer called barrier layer and a porous outer layer called honeycomb. This porosity is obtained by the chemical dissolution of the oxide layer over time which causes the increase of pore diameters.

C. Influence of the Thickness of the Oxide Layer on the Coefficient of Friction

Figure 3 shows the coefficient of friction (μ) of a sample with $9.5 \mu\text{m}$ thickness measured with the scratch test. To confirm the obtained value of the coefficient of friction, two scratch tests were conducted. The obtained value is of the order of 0.3 and 0.35. Figure 4 shows the coefficient of friction of sample 2 with $12 \mu\text{m}$ thickness. The values obtained by the scratch test range between 0.5 and 0.55. From these values, it is

found that the increase in the anodizing time allows getting a higher μ . Therefore, it can be concluded, that the thickness of the oxide layer influences the coefficient of friction of the oxide layer obtained by the scratch test. The increase in the coefficient of friction is due to the increase in the pore diameter of the oxide layer. Authors in [29] carried out an immersion magnification treatment of anodized samples under different durations and they found that a long anodizing duration has a great impact on the friction level. Authors in [30] carried out wear tests and showed that the variation of the coefficient of friction depends on the morphology of the oxide layer. They reported that the coefficient of friction tends to increase with increasing pore size.

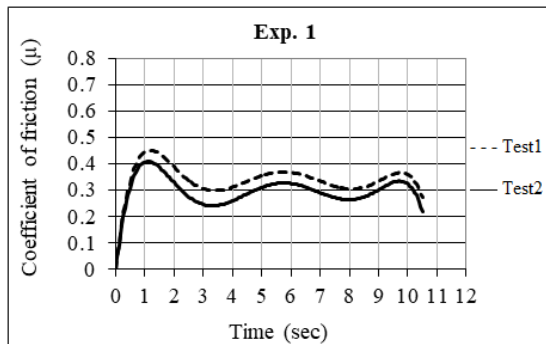


Fig. 3. Coefficient of friction for sample 1.

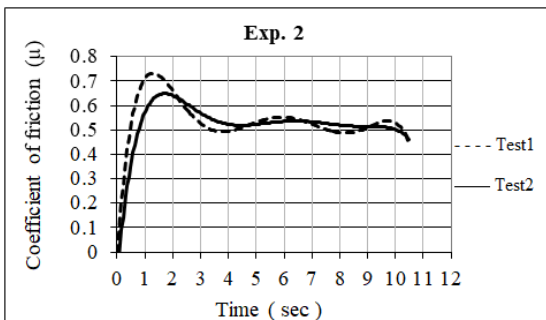


Fig. 4. Coefficient of friction for sample 2.

D. Influence of the Applied Current on the Tribological Behavior of the Oxide Layer

The main role of the current applied during anodizing treatment is to increase the reaction speed in order to ensure the movement of the electrons between the anode and the cathode in the electrolyte bath. The variation of the applied current has an important influence on the tribological properties of the oxide layer. In our case, two applied currents of anodizing treatment were studied and the wear resistance of the alumina layer was analyzed. Figure 5 presents the evolution of the friction coefficient of sample 1. The average friction coefficient of the specimen of 1 A/dm^2 applied current is 0.55. The frictional response throughout the tribological characterization test. Furthermore, according to Figure 6, showing the SEM observations of the friction scar of the sample 1 with different magnifications, the oxide layer is completely removed, which

confirms the result of Figure 5. The cyclic friction test induces the formation of the wear particles which is composed of the alloy of aluminum and the alumina layer. In addition, the wear fragment is compacted on the surface of the substrate (Figure 6(b)).

Figure 7 shows the evolution of the coefficient of friction of the sample 2 with a variation of the applied current density from 1 A/dm^2 to 2 A/dm^2 . Sample 2 has a low friction coefficient of the order of 0.3 for the first 30 cycles. Then it gradually increases with a slight slope to reach a value of 0.8 before stabilizing after 75 cycles. Hence, it is clear that the wear resistance of the oxide layer varies with the applied current, as it is greater for an applied current density of 2 A/dm^2 than for 1 A/dm^2 . Figure 8 displays the SEM observations with different magnifications. These images show that there is a partial detachment of the oxide layer (Figure 8(a)) from the substrate with the formation of the micrometric wear particles of varying sizes (Figure 8(c)). The wear debris is compacted on the surface, forming a smoother scar that fills the porosity of the oxide layer. In addition, vertical cracks perpendicular to the direction of friction appear at the wear scar (Figure 8(b)). The compacted wear particle is responsible for the increments of the friction coefficient after 30 cycles since the surface becomes smooth.

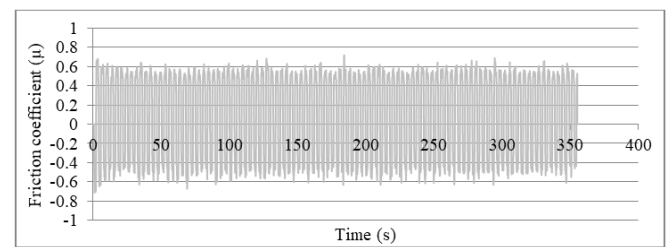


Fig. 5. Evolution of the friction response under cyclic test- sample 1.

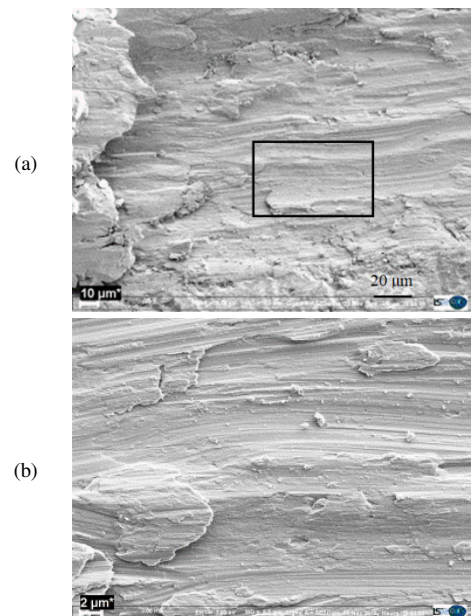


Fig. 6. (a) Post process analysis of sample 1: (a) $1 \text{ A/dm}^2 + 100 \text{ g/l}$, (b) corresponding detail of the framed zone of (a).

When they studied the effect of reaction time on the cyclic behavior of the 5083 aluminum alloy oxide layer, authors in [31] reported that increasing the RT improved the durability of the material. In addition, when RT increased, the stability of the friction coefficient was improved and the pores on the surface were further filled with micro-sized wear particles, inducing the establishment of a compacted layer. Therefore, the 5083 aluminum alloy oxide layer shows a similar behavior to the reference 2017A T4, and has important tribological characteristics such as durability and wear resistance after hundreds of friction cycles. Authors in [29, 30] found that the variation of the friction coefficient depends on the morphology of the oxide layer and that this coefficient tends to increase with increasing pore size.

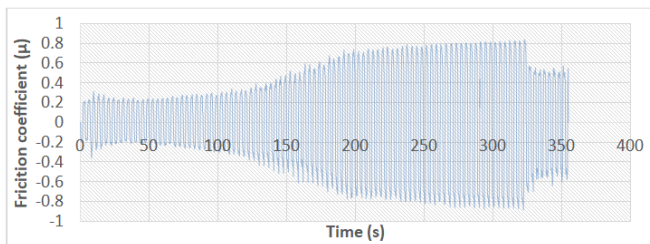


Fig. 7. Evolution of the friction response using cyclic friction test of sample 2.

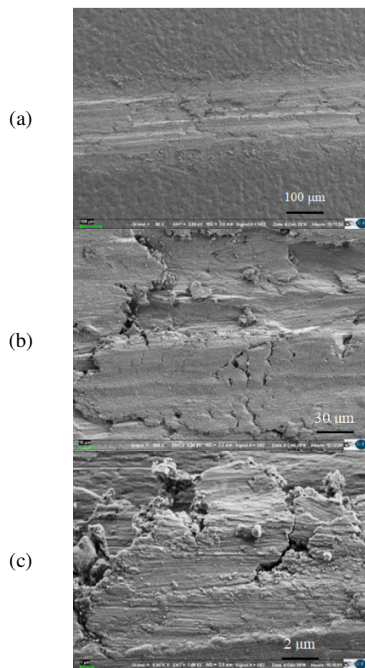


Fig. 8. SEM image of the wear mechanisms obtained by the cyclic friction test for the sample 2: (a) 2 A/dm². (b), (c) higher magnification images of (a).

E. Influence of the Applied Current and the Electrolyte Concentration on the Tribological Behavior of the Oxide Layer

A simultaneous increase in the applied current and concentration was studied in sample 3. Figure 9 shows the friction response of the fourth cyclic friction test with an

increase of the concentration from 100 g/l to 200 g/l and a variation of the applied current density from 1 A/dm² to 2 A/dm². The high conductivity coupled with the acceleration of the anodizing reaction gives the most stable response with a low friction coefficient. The obtained friction coefficient is of the order of 0.34. This value is very close to that of the first 30 cycles of the friction test of sample 2. The SEM microscope observation of the damage morphology with different magnifications (Figure 10) shows that during the cyclic friction test the oxide layer stands 100 cycles. Indeed, the alumina layer does not wear off and there is no penetration of the substrate (Figure 10(b)). At higher magnification (Figure 10(c)), vertical and horizontal fatigue cracks appear in the wear scar, which explains the great hardness of the anodized surface. This finding confirms the good stability and the value of the friction coefficient. Therefore, after the comparative study performed in this article, the last sample has a high resistance to abrasion and wear.

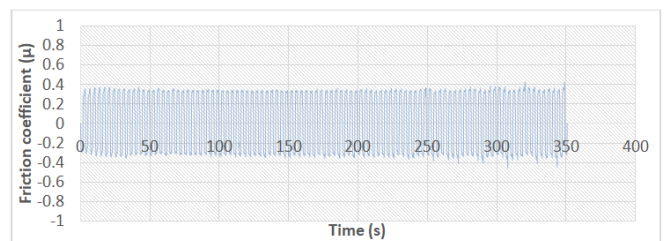


Fig. 9. Curve of the friction response using cyclic friction test of sample 3.

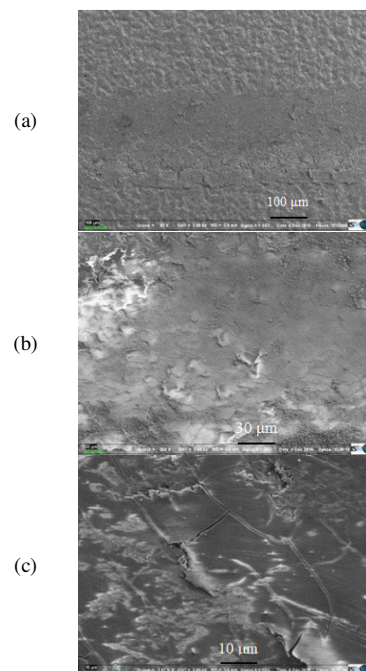


Fig. 10. SEM images of the wear mechanisms obtained by the cyclic friction test for the sample 3: (a) 2 A/dm², (b)-(c) higher magnification images of (a).

IV. CONCLUSION

The friction behavior of the aluminum alloy 2017A was studied on relation to the effect of anodic oxide layer thickness which is controlled by the anodizing potential. Two durations of anodization, 30 and 60 min, were particularly examined. Based on the present experiments, the following conclusions are drawn:

- The variation of the anodizing duration has a marked effect on the thickness of the oxide layer.
- Longer anodizing duration yielded thicker and harder aluminum oxide coating.
- The increase in the thickness of the anodic oxide layer increases the coefficient of friction.
- Variations in coefficient of friction with sliding distance are influenced by changes in wear morphology and degree of oxidation. The treated surfaces with a thickness of 50 μm have the lowest friction coefficients and wear rates. Their improved wear resistance may be related to the increased bond strength compared to other anodized surfaces.
- The tribological damage was characterized by the detachment of debris, which increases with the increase of the duration of anodization. Upon sliding, its detachment leads to delamination of the underlying anodic aluminum oxides and subsequent abrasion of the aluminum substrate.

ACKNOWLEDGEMENT

The author is thankful to the deanship of scientific research at the University of Bisha for supporting this work through the fast-track research support program. Specific thanks are allocated to the LSPM, LGM, and LASEM laboratories for sample characterization, and SIAC company for the materials.

REFERENCES

- [1] A. P. Mouritz, *Introduction to Aerospace Materials*. Sawston, UK: Woodhead, 2012.
- [2] A. S. H. Makhlof and M. Aliofkhaezrai, *Handbook of Materials Failure Analysis with Case Studies from the Aerospace and Automotive Industries*. Oxford, UK: Butterworth-Heinemann, 2015.
- [3] O. Bildik and M. Yasar, "Manufacturing of Wear Resistant Iron-Steel: A Theoretical and Experimental Research on Wear Behavior," *Engineering, Technology & Applied Science Research*, vol. 11, no. 3, pp. 7251–7256, Jun. 2021, <https://doi.org/10.48084/etasr.4092>.
- [4] M. Ramadan, "Interface Structure and Elements Diffusion of As-Cast and Annealed Ductile Iron/Stainless Steel Bimetal Castings," *Engineering, Technology & Applied Science Research*, vol. 8, no. 2, pp. 2709–2714, Apr. 2018, <https://doi.org/10.48084/etasr.1856>.
- [5] D. Blanco, E. M. Rubio, M. M. Marin, and J. P. Davim, "Advanced materials and multi-materials applied in aeronautical and automotive fields: a systematic review approach," *Procedia CIRP*, vol. 99, pp. 196–201, Jan. 2021, <https://doi.org/10.1016/j.procir.2021.03.027>.
- [6] W. Rajhi, "Numerical Simulation of Damage on Warm Deep Drawing of Al 6061-T6 Aluminium Alloy," *Engineering, Technology & Applied Science Research*, vol. 9, no. 5, pp. 4830–4834, Oct. 2019, <https://doi.org/10.48084/etasr.3148>.
- [7] N. Altinkok, I. Ozsert, and F. Findik, "Dry Sliding Wear Behavior of Al₂O₃/SiC Particle Reinforced Aluminium Based MMCs Fabricated by Stir Casting Method," *Acta Physica Polonica A*, vol. 124, no. 1, pp. 11–19, 2013, <https://doi.org/10.12693/APhysPolA.124.11>.
- [8] T. Doksanovic, I. Dzeba, and D. Markulak, "Variability of structural aluminium alloys mechanical properties," *Structural Safety*, vol. 67, pp. 11–26, Jul. 2017, <https://doi.org/10.1016/j.strusafe.2017.03.004>.
- [9] E. Dervishi *et al.*, "Mechanical and tribological properties of anodic Al coatings as a function of anodizing conditions," *Surface and Coatings Technology*, vol. 444, Aug. 2022, Art. no. 128652, <https://doi.org/10.1016/j.surfcoat.2022.128652>.
- [10] M. Guezmil, W. Bensalah, A. Khalladi, K. Elleuch, M. De-Petris Wery, and H. F. Ayedi, "Effect of Test Parameters on the Friction Behaviour of Anodized Aluminium Alloy," *International Scholarly Research Notices*, vol. 2014, Oct. 2014, Art. no. 795745, <https://doi.org/10.1155/2014/795745>.
- [11] R. J. H. Wanhill, "Fatigue crack initiation in aerospace aluminium alloys, components and structures," National Aerospace Laboratory, Amsterdam, Netherlands, Technical Report NLR-TP-2006-751, 2007.
- [12] K. Anderson, J. Weritz, and J. G. Kaufman, *ASM Handbook: Aluminum science and technology*, vol. 2A. Almere, Netherlands: ASM International, 2018.
- [13] D. Jacquin and G. Guillemot, "A review of microstructural changes occurring during FSW in aluminium alloys and their modelling," *Journal of Materials Processing Technology*, vol. 288, Feb. 2021, Art. no. 116706, <https://doi.org/10.1016/j.jmatprotec.2020.116706>.
- [14] M. Shahzad, M. Chaussumier, R. Chieragatti, C. Mabru, and F. Reza-Aria, "Influence of anodizing process on fatigue life of machined aluminium alloy," *Procedia Engineering*, vol. 2, no. 1, pp. 1015–1024, Apr. 2010, <https://doi.org/10.1016/j.proeng.2010.03.110>.
- [15] F. Findik, "Latest progress on tribological properties of industrial materials," *Materials & Design*, vol. 57, pp. 218–244, May 2014, <https://doi.org/10.1016/j.matdes.2013.12.028>.
- [16] J. Korzekwa, M. Fal, and A. Gadek-Moszczak, "DOE Application for Analysis of Tribological Properties of the Al₂O₃/IF-WS₂ Surface Layers," *Open Engineering*, vol. 11, no. 1, pp. 171–181, Jan. 2021, <https://doi.org/10.1515/eng-2021-0012>.
- [17] G. Patermarakis, "Thorough electrochemical kinetic and energy balance models clarifying the mechanisms of normal and abnormal growth of porous anodic alumina films," *Journal of Electroanalytical Chemistry*, vol. 730, pp. 69–85, Sep. 2014, <https://doi.org/10.1016/j.jelechem.2014.07.034>.
- [18] M. Sieber, R. Morgenstern, and T. Lampke, "Anodic oxidation of the AlCu4Mg1 aluminium alloy with dynamic current control," *Surface and Coatings Technology*, vol. 302, pp. 515–522, Sep. 2016, <https://doi.org/10.1016/j.surfcoat.2016.06.043>.
- [19] M. Bononi, R. Giovanardi, A. Bozza, and P. Mattioli, "Pulsed current effect on hard anodizing process of 2024-T3 aluminium alloy," *Surface and Coatings Technology*, vol. 289, pp. 110–117, Mar. 2016, <https://doi.org/10.1016/j.surfcoat.2016.01.056>.
- [20] J. Lu, G. Wei, Y. Yu, C. Guo, and L. Jiang, "Aluminum alloy AA2024 anodized from the mixed acid system with enhanced mechanical properties," *Surfaces and Interfaces*, vol. 13, pp. 46–50, Dec. 2018, <https://doi.org/10.1016/j.surf.2018.08.003>.
- [21] K. Dejun, W. Jinchun, and L. Hao, "Friction and Wear Performances of 7475 Aluminium Alloy after Anodic Oxidation," *Rare Metal Materials and Engineering*, vol. 45, no. 5, pp. 1122–1127, May 2016, [https://doi.org/10.1016/S1875-5372\(16\)30105-9](https://doi.org/10.1016/S1875-5372(16)30105-9).
- [22] M. Sarraf, B. Nasiri-Tabrizi, A. Dabbagh, W. J. Basirun, and N. L. Sukiman, "Optimized nanoporous alumina coating on AA3003-H14 aluminum alloy with enhanced tribo-corrosion performance in palm oil," *Ceramics International*, vol. 46, no. 6, pp. 7306–7323, Apr. 2020, <https://doi.org/10.1016/j.ceramint.2019.11.227>.
- [23] M. Remesova *et al.*, "Effects of anodizing conditions and the addition of Al₂O₃/PTFE particles on the microstructure and the mechanical properties of porous anodic coatings on the AA1050 aluminium alloy," *Applied Surface Science*, vol. 513, May 2020, Art. no. 145780, <https://doi.org/10.1016/j.apsusc.2020.145780>.
- [24] S. H. Mohitfar, S. Mahdavi, M. Etminanfar, and J. Khalil-Allafi, "Characteristics and tribological behavior of the hard anodized 6061-T6 Al alloy," *Journal of Alloys and Compounds*, vol. 842, Nov. 2020, Art. no. 155988, <https://doi.org/10.1016/j.jallcom.2020.155988>.

- [25] M. Niedzwiedz, W. Skoneczny, and M. Bara, "The influence of anodic alumina coating nanostructure produced on EN AW-5251 alloy on type of tribological wear process," *Coatings*, vol. 10, no. 2, 2020, Art. no. 105, <https://doi.org/10.3390/coatings10020105>.
- [26] M. Niedzwiedz, M. Bara, W. Skoneczny, S. Kaptacz, and G. Dercz, "Influence of Anodizing Parameters on Tribological Properties and Wettability of Al₂O₃ Layers Produced on the EN AW-5251 Aluminum Alloy," *Materials*, vol. 15, no. 21, Nov. 2022, Art. no. 7732, <https://doi.org/10.3390/ma15217732>.
- [27] *ASTM B244-09(2014), Standard Test Method for Measurement of Thickness of Anodic Coatings on Aluminum and of Other Nonconductive Coatings on Nonmagnetic Basis Metals with Eddy-Current Instruments*. West Conshohocken, PA, USA: ASTM International, 2014.
- [28] G. C. Wood and J. P. O'Sullivan, "The anodizing of aluminium in sulphate solutions," *Electrochimica Acta*, vol. 15, no. 12, pp. 1865–1876, Dec. 1970, [https://doi.org/10.1016/0013-4686\(70\)85024-1](https://doi.org/10.1016/0013-4686(70)85024-1).
- [29] M. Guezmil, W. Bensalah, A. Khalladi, K. Elleuch, M. Depetris-wery, and H. F. Ayedi, "Friction coefficient and microhardness of anodized aluminum alloys under different elaboration conditions," *Transactions of Nonferrous Metals Society of China*, vol. 25, no. 6, pp. 1950–1960, Jun. 2015, [https://doi.org/10.1016/S1003-6326\(15\)63803-1](https://doi.org/10.1016/S1003-6326(15)63803-1).
- [30] H. Kim, D. Kim, W. Lee, S. J. Cho, J.-H. Hahn, and H.-S. Ahn, "Tribological properties of nanoporous anodic aluminum oxide film," *Surface and Coatings Technology*, vol. 205, no. 5, pp. 1431–1437, Nov. 2010, <https://doi.org/10.1016/j.surfcoat.2010.07.056>.
- [31] M. Abid, M. Kchaou, A. T. Hoang, and M. Haboussi, "Wear Mechanisms Analysis and Friction Behavior of Anodic Aluminum Oxide Film 5083 under Cyclic Loading," *Journal of Materials Engineering and Performance*, Aug. 2023, <https://doi.org/10.1007/s11665-023-08616-8>.